Shibuya *et al. Progress in Earth and Planetary Science* (2015) 2:46
DOI 10.1186/s40645-015-0076-z

Progress in Earth and Planetary Science
a SpringerOpen Journal

RESEARCH ARTICLE Open Access

Hydrogen-rich hydrothermal environments in the Hadean ocean inferred from serpentinization of komatiites at 300 °C and 500 bar

Takazo Shibuya[1,2,3*], Motoko Yoshizaki[4], Masahiko Sato[5], Kenji Shimizu[2,6], Kentaro Nakamura[7], Soichi Omori[8], Katsuhiko Suzuki[2,3], Ken Takai[1,2,3,9], Hideo Tsunakawa[4] and Shigenori Maruyama[4,10]

Abstract

Serpentinization of Al-depleted and Al-undepleted komatiites (and olivine for comparison) was experimentally characterized under high-temperature and high-pressure conditions of 300 °C and 500 bar to evaluate the H_2 generation potential in komatiite-hosted hydrothermal systems in the early Earth. From the results, the steady-state H_2 concentrations of fluids were estimated to be approximately 20 and 0.05 mmol/kg during the serpentinization reactions for Al-depleted and Al-undepleted komatiites, respectively (60 mmol/kg in the case of olivine). The H_2 concentration of hydrothermal fluid generated from the serpentinization of Al-depleted komatiite is lower than that from olivine but is comparable to that of typical modern peridotite-hosted hydrothermal systems (~16 mmol/kg). The relatively low H_2 concentration from Al-undepleted komatiite is similar to the levels in modern basalt-hosted hydrothermal fluids. Considering that the generation of Al-depleted komatiite melt requires a hotter mantle upwelling (plume) than the generation of Al-undepleted komatiite melt and that the temperature of the mantle has gradually decreased throughout Earth's history, Al-depleted komatiite may have constituted ultramafic volcanism in Hadean oceanic islands/plateaus. Furthermore, it seems unlikely that seafloor exposure of mantle peridotites occurred frequently in the Hadean because the oceanic crust of that time was presumably much thicker than the modern equivalent. Therefore, the serpentinization of Al-depleted komatiites may have been the main process that provided abundant H_2-rich seafloor hydrothermal environments in the Hadean ocean, which potentially acted as a nursery for the prebiotic chemical evolution and the emergence and early evolution of life on Earth.

Keywords: Serpentinization, Komatiite, Hydrogen, Hydrothermal fluid, Hydrothermal experiment, Hadean, Origin of life, Early evolution of life

Background

Serpentinization of seafloor ultramafic rocks is one of the most important geological processes that could have been involved in the emergence and early evolution of life on Earth. During serpentinization, molecular hydrogen (H_2) is characteristically generated by the reaction of water with ferrous oxide in rocks. This process would have sustained H_2-rich seafloor hydrothermal environments where organic materials necessary for the emergence of life could have been synthesized and preserved (Amend and McCollom 2009), and energetically preferred catabolic and anabolic metabolisms of early life could have been established (Takai et al. 2006; Martin et al. 2008; Shibuya et al. 2010; Russell et al. 2014; Sleep et al. 2011).

In modern oceans, serpentinization of ultramafic rocks and the resulting H_2-rich hydrothermal activity often occur in slow-spreading ridges without sufficient magmatic supply, such as the Mid-Atlantic Ridge (MAR)

---

* Correspondence: takazos@jamstec.go.jp
[1] Laboratory of Ocean-Earth Life Evolution Research (OELE), Japan Agency for Marine-Earth Science and Technology (JAMSTEC), 2-15 Natsushima-cho, Yokosuka 237-0061, Japan
[2] Research and Development (R&D) Center for Submarine Resources, Japan Agency for Marine-Earth Science and Technology (JAMSTEC), 2-15 Natsushima-cho, Yokosuka 237-0061, Japan
Full list of author information is available at the end of the article

(Charlou et al. 2002) and the Central Indian Ridge (Kumagai et al. 2008; Nakamura et al. 2009; Morishita et al. 2015) and exceptionally in off-axis mantle-exposed regions such as the Lost City hydrothermal field away from the MAR (Kelley et al. 2001, 2005; Lang et al. 2010). These peridotite-associated hydrothermal systems have been a subject of great research interest because of their geological, geochemical, and biological uniqueness in comparison with conventional basalt-hosted mid-ocean ridge hydrothermal systems (Takai et al. 2006; Nakamura and Takai 2014). Furthermore, an experiment simulating hydrothermal reactions between peridotite and seawater also revealed the great potential of serpentinization to generate H_2-rich hydrothermal fluid (Seyfried et al. 2007). Therefore, such peridotite-associated hydrothermal systems have been perceived as modern analogues of the Hadean ultramafic-hosted systems that could have been possible nurseries for the emergence and early evolution of life.

In the early Earth, the oceanic crust was likely much thicker (approximately three times thicker) than the modern equivalent (6–7 km thickness) owing to the hotter mantle at that time and has become thinner as the temperature of the mantle has decreased with time, as suggested by the geological occurrence of ophiolites (Moores 2002) and the compositional evolution of greenstones derived from mid-ocean ridges (Komiya 2004). Therefore, it has been theoretically hypothesized that the thick lid of oceanic crust probably limited exposure of mantle peridotite on the seafloor; thus, komatiite rather than peridotite would have been the predominant ultramafic rock in the early Archean ocean floor (Takai et al. 2006). Regarding the genesis of komatiite, there was a controversy as to whether komatiites were derived from wet or dry mantle (Arndt et al. 1998; Grove and Parman 2004) since komatiites were first recognized by Viljoen and Viljoen (1969). It is now known that komatiites can be generated not only by high-temperature and high-pressure partial melting in dry mantle (Takahashi and Scarfe 1985) but also under much lower temperature and pressure conditions in hydrous mantle plumes (Inoue and Sawamoto 1992; Inoue et al. 2000). Grove and Parman (2004) even interpreted komatiites as being formed by shallow-level melting of hydrous mantle wedge above subduction zone. However, the low water contents in komatiitic melt inclusions (Shimizu et al. 2001; Berry et al. 2008) and the similar oxygen fugacity of komatiite magmas to the modern normal upper mantle (Canil 1997, 1999; Puchtel et al. 2013) are not consistent with the hydrous melting model. Therefore, most researchers have agreed that komatiites were produced by extraordinarily hot melting in mantle upwellings (plumes) under nearly dry conditions (e.g., Takahashi and Scarfe 1985; Campbell et al. 1989; Herzberg et al. 2010).

Furthermore, Archean komatiites have generally been classified into two types by their Al_2O_3 content, such as Al-depleted (Barberton-type) and Al-undepleted (Munro-type) komatiites, which mainly occur in the early and late Archean greenstone belts, respectively (Nesbitt et al. 1979). Melting experiments under dry conditions revealed that Al-depleted komatiite (ADK) was formed by high-temperature, ultra-deep, high-degree mantle partial melting, whereas Al-undepleted komatiite (AUK) was generated under relatively lower pressure and temperature conditions than ADK (e.g., Wei et al. 1990; Herzberg 1992). Therefore, this compositional change of komatiite likely reflects the decrease in mantle temperature through geologic time (Herzberg et al. 2010).

Of course, komatiite-associated hydrothermal activity does not occur in the modern ocean; thus, the H_2 generation potential of komatiites during serpentinization can only be experimentally estimated through simulated hydrothermal fluid–rock reactions under high-temperature and high-pressure conditions, as previously conducted to reconstruct modern (Seyfried 1987; Seyfried et al. 2007; McCollom et al. 2010; Kato et al. 2013; Suzuki et al. 2015a, b), ancient (Yoshizaki et al. 2009; Lazar et al. 2012; Shibuya et al. 2013), and even extraterrestrial subseafloor hydrothermal systems (Hsu et al. 2015; Sekine et al. 2015). Yoshizaki et al. (2009) confirmed hydrogen generation by a preliminary, ongoing experiment using komatiite and pure water (Yoshizaki et al. 2009). However, the H_2 generation potential of not only ADK but also AUK, during serpentinization, has not yet been evaluated by completed experiments.

In this study, we conducted experiments to simulate the reactions between komatiite and seawater (NaCl solution) at 300 °C and 500 bar, using a batch-type (closed system) hydrothermal reactor (Yoshizaki et al. 2009). For these experiments, both ADK and AUK were prepared to ascertain the H_2 generation potential in komatiite-hosted hydrothermal system through geologic time. The results allowed us to estimate the H_2 concentration of hydrothermal fluids in Hadean komatiite-hosted hydrothermal systems, which can be used to obtain further insights into the possible energetics and kinetics of prebiotic chemical evolution and the emergence and early evolution of life on the early Earth.

Methods

Preparation of the starting solid materials

Olivine (San Carlos) and two types of synthetic komatiite were prepared for use as the starting solid materials in the experiments. Two types of komatiites were synthesized from reagents. The composition of the reagent powders was adjusted to produce synthetic Al-depleted (Al_2O_3 = c. 5 wt%) and Al-undepleted (Al_2O_3 = c. 10 %) komatiites based on the compositions of natural ADK and AUK (Arth et al. 1977; Wei et al. 1990) (Table 1).

Table 1 Composition of the starting materials used in the experiments and the natural Al-depleted and Al-undepleted komatiites (wt%)

	Starting material			Natural komatiite			
	Olivine[a]	Al_2O_3-5 % komatiite[b]	Al_2O_3-10 % komatiite[b]	ADK[c]	ADK[d]	AUK[e]	AUK[f]
SiO_2	41.25	46.92	44.30	46.50	47.16	45.90	48.96
TiO_2	0.01	0.30	0.29	0.30	0.38	0.41	0.47
Al_2O_3	0.02	4.78	10.11	4.74	4.09	7.97	9.87
FeO_{total}	9.20	11.16	10.53	11.90	12.01	11.07	10.96
MnO	0.10	0.21	0.20	0.21	0.20	0.21	0.19
MgO	49.92	29.61	27.95	29.30	27.97	26.38	19.50
CaO	0.09	6.55	6.19	6.32	6.61	7.74	8.91
Na^2O	0.01	0.35	0.33	0.35	0.37	0.43	1.06
K_2O	0.00	0.11	0.11	0.11	0.04	0.09	0.08

[a] Determined by EPMA analysis

[b] Calculated from the amounts of reagents

[c] An Al-depleted komatiite collected from Barbertone Greenstone Belt (South Africa) (Yoshizaki et al. 2009)

[d] An average composition of Al-depleted komatiites from Barbertone greenstone belt (South Africa) (Wei et al. 1990)

[e] An average composition of Al-undepleted komatiites from Munro/Newton Township (Canada) and Belingwe greenston belt (Zimbabwe) (Wei et al. 1990)

[f] An average composition of Al-undepleted komatiites from Munro Township (Canada) (Arth et al., 1977)

Approximately 30 g of sample powder was placed in a Pt-Rh crucible and heated at 1000 °C for 1 h in an electric furnace to decarbonate the initial reagents. Subsequently, the sample was fused at 1600 °C for 1 h while regulating oxygen fugacity at a QFM (quartz–fayalite–magnetite) buffer under an H_2–CO_2 mixed gas atmosphere. To create the spinifex texture of olivine, the temperature was lowered to 1450 °C over 1.5 h and then to 1350 °C over 18 h under QFM conditions, after which the sample was immediately quenched, yielding a fresh komatiite.

The San Carlos olivine crystals and synthesized olivine-spinifex komatiite (with minor spinel phase) was crushed in a tungsten mortar and sieved to obtain the <90 μm fraction. To remove possible contamination by organic matter during sample preparation, the powdered komatiite was ultrasonically washed with acetone and pure water several times and then dried at 50 °C for 12 h prior to the experiment. The composition of olivine was determined using an electron probe microanalyzer, and the composition of synthetic komatiites was also confirmed using X-ray fluorescence.

Experimental system

An autoclave based on Seyfried et al. (1979) was used for the hydrothermal reaction experiment in this study. The autoclave is made of Inconel-alloy, which is corrosion-resistant and possesses adequate strength at elevated temperatures and pressures of up to 600 °C and 600 bar, respectively (Fig. 1; modified after Yoshizaki et al. 2009). The reaction cell is made of a gold bag with a titanium head because these materials are inert with respect to high-temperature water. In addition, as gold is flexible, the water inside the reaction cell can be pressurized by the surrounding water. Although the Ti head is corrosion-resistant, it is known that metallic Ti can react with water to produce hydrogen; thus, the surface of the Ti head was oxidized prior to use. The flexible gold reaction cell allows on-line sampling of the aqueous fluid at almost constant temperature and pressure simply by adding a small amount of pressurized water to the space surrounding the reaction cell in the autoclave. In this way, fluid samples can be obtained from the reaction cell through a gold-lined sampling tube at any time during an ongoing experiment. All materials that would come into contact with the reaction fluid in the experiment were

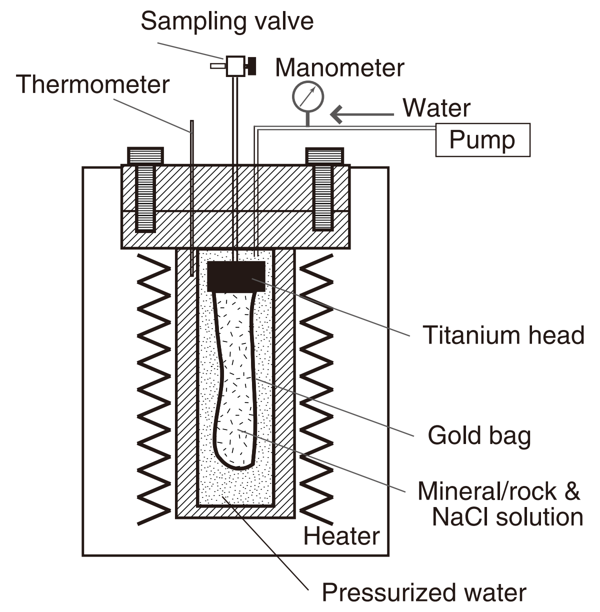

Fig. 1 Schematic of the hydrothermal reactor used in this study, modified after Yoshizaki et al. (2009)

baked in a muffle furnace at 500 °C for 3 h prior to use to eliminate organic matter.

The NaCl solution (approximately 6–7 mol/kg) was prepared from NaCl and pure water to simulate the Hadean seawater, which was potentially saltier than that of the present day owing to the absence of continental crust and associated salt deposits in the Hadean (Knauth 2005). To avoid contamination with organic matter, the NaCl was baked prior to use. The water/rock mass ratio was adjusted to four at the beginning of the experiment (approximately 60 g of solution and 15 g of rock powder) based on the results of Wetzel and Shock (2000) that the water/rock mass ratio in the high-temperature region in the subseafloor hydrothermal system is limited to values less than five. The overall background level of hydrogen concentration in hydrothermal fluid is lower than 0.002 mmol/kg, which was estimated from a 3-month experiment using pure silica powder and NaCl solution under the same temperature and pressure conditions.

Sampling and analysis

Fluid samples were obtained from the reaction cell through a gold-lined sampling tube several times during the ongoing experiment. For the analysis of H_2 concentration, approximately 0.5 ml of fluid was directly introduced into an Ar-purged, sealed vial without air contamination at room temperature. After equilibration between gas and liquid phases in the vial, the H_2 concentration in the gas phase was quantitatively analyzed by gas chromatography (GC) at JAMSTEC. The analytical reproducibility was better than 5 % (1σ). The solid materials of alteration products were dried in an oven immediately after the experiments and then preserved in a vacuum desiccator. The alteration products were analyzed by X-ray diffraction (XRD) at JAMSTEC and by a magnetometer (see below) after the experiment.

Magnetic measurements

For the starting solid material and alteration product of the experiments with olivine, Al_2O_3-5 %, and Al_2O_3-10 % komatiites, the magnetic hysteresis loops at room temperature were measured to estimate the amount of magnetite generated through the experiments using a MicroMag 2900 Alternating Gradient Magnetometer (AGM, Princeton Measurements Corporation) at Kyushu University with a maximum field of 500 mT. The strong-field thermomagnetic curve of the alteration product of the olivine experiment was measured between 50 °C and 780 °C using a MicroMag 3900 Vibrating Sample Magnetometer (VSM, Princeton Measurements Corporation) at the Tokyo Institute of Technology. The magnetic hysteresis loops at low temperatures (10, 15, 20, 25, 30, 35, 40, 45, 50, 55, 60, and 65 K) were measured for the starting materials and alteration products of the komatiite experiments using an MPMS-XL5 Magnetic Property Measurement System (MPMS, Quantum Design) at the Center for Advanced Marine Core Research (CMCR), Kochi University. In the low-temperature measurements, the maximum field in the hysteresis loop measurement was set to be 3 T.

Results and discussion

The powdered olivine, Al_2O_3-5 %, and Al_2O_3-10 % komatiites were reacted with NaCl solution at 300 °C and 500 bar for 2112–2688 h to assess their H_2 generation potential in seafloor hydrothermal systems. In this section, we discuss the alteration of solid materials and its relation to the H_2 concentration in hydrothermal fluid, which yields implications for H_2-rich hydrothermal environments in the Hadean ocean.

Alteration products

The XRD analyses of the alteration products revealed that all the experiments generated a certain amount of serpentine during the hydrothermal reactions (Fig. 2), indicating that serpentinization occurred during these experiments. However, peaks of smectite were observed in the alteration products after the experiments with both Al_2O_3-5 % and Al_2O_3-10 % komatiites. The peaks of smectite in the alteration products were larger for Al_2O_3-10 % komatiite than for Al_2O_3-5 % komatiite; this suggests that smectite becomes more stable as the Al_2O_3 content of the starting material is increased. In addition, CaO originally contained in the starting material of both komatiites was converted to xonotlite.

In general, H_2 generation during serpentinization is caused by the reduction of water as a result of oxidation of ferrous iron in fresh ultramafic rocks (e.g., Janecky and Seyfried 1986). This process can be written as

$$2(\mathrm{FeO})_{\mathrm{rock}} + \mathrm{H_2O} \rightarrow (\mathrm{Fe_2O_3})_{\mathrm{rock}} + \mathrm{H_2},$$

where $(FeO)_{rock}$ refers to the ferrous oxide component in silicate minerals (and glass) while $(Fe_2O_3)_{rock}$ indicates the ferric oxide component of minerals in a serpentinized rock (e.g., McCollom and Bach 2009). Because the ferric oxide typically precipitates as magnetite (ferric/ferrous oxide: Fe_3O_4), the amount of magnetite generated through reactions is strongly related to the H_2 concentration in hydrothermal fluid. In the XRD analyses of the alteration products, no clear peaks of magnetite were identified owing to its small quantities (below the detection limit). However, the magnetic measurements provided constraints on the amounts of effective magnetite generated in the experiments. Figure 3 shows the hysteresis loops of the starting material and alteration product of all experiments. From the hysteresis loops, the saturation magnetization (M_s) values were also

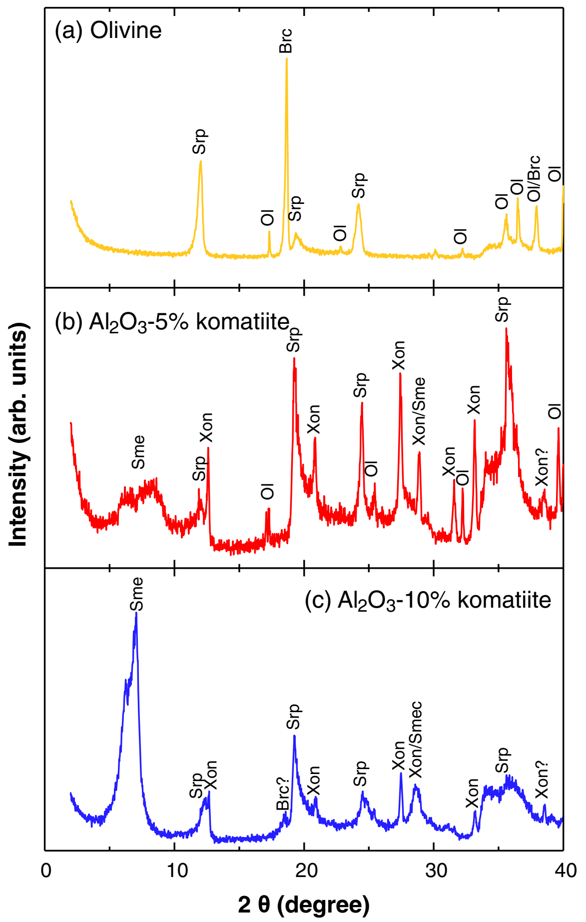

Fig. 2 Results of the XRD analysis (CuKα) of the alteration products. XRD pattern of the alteration products from the experiments with (**a**) olivine, (**b**) Al_2O_3-5 % komatiite, and (**c**) Al_2O_3-10 % komatiite. Mineral abbreviations and ideal chemical formula: Ol = olivine ($(Mg, Fe)_2SiO_4$), Sme = smectite ($(Na, Ca)_{03}(Al, Fe, Mg)_{2-3}(Si, Al)_4O_{10}(OH)_2 \cdot nH_2O$), Srp = serpentine ($(Mg, Fe)_3Si_2O_5(OH)_4$), Brc = brucite ($(Mg, Fe)(OH)_2$), and Xon = xonotlite ($Ca_6Si_6O_{17}(OH)_2$)

calculated (Table 2). In the olivine experiment, the M_s values of the alteration product and starting material were estimated from the room-temperature hysteresis loops to be 3.69 Am^2/kg and less than 0.01 Am^2/kg, respectively (Fig. 3a, b, and Table 2). Furthermore, the strong-field thermomagnetic curve of the alteration product of the olivine experiment shows that the Curie temperature (T_C) was 538 °C (Fig. 4a), indicating the formation of nearly pure magnetite during the experiment. Using the well-known magnetite M_s value of 92 Am^2/kg (Hunt et al. 1995), the alteration product of the olivine experiment is estimated to contain 4.0 wt% magnetite.

In both komatiite experiments, the M_s values of the starting material and alteration product were less than 0.05 Am^2/kg at room temperature (Table 2), which indicates that these solid materials contain no or only minute quantities of ferromagnetic minerals with T_C higher than room temperature. In contrast, the M_s values calculated from the hysteresis loops measured at 10 K for these samples were greater than 0.80 Am^2/kg (Fig. 3c–f, Table 2). These results revealed that the solid materials mainly contained a magnetic mineral with T_C lower than room temperature. The temperature dependences of M_s were also calculated from their hysteresis loops (Fig. 4b), which yielded T_C values of these materials of approximately 30 K. Although it is difficult to determine the composition of these magnetic minerals, the most probable candidate with a T_C value of approximately 30 K is a solid solution between magnetite and spinel phases such as $(Fe_3O_4)_x(MgAl_2O_4)_{1-x}$ (Harrison and Putnis 1996). The starting materials showed a certain level of M_s value (Table 2), which is consistent with the starting materials originally containing spinel. In addition, the normalized M_s of the starting material of the Al_2O_3-5 % komatiite experiment is slightly higher than that of the alteration product at temperatures above 30 K (Fig. 4b), indicating that a tiny amount of magnetite is probably contained in the starting material in addition to the magnetite–spinel solid solution. On the other hand, the M_s values of the alteration products are clearly higher than those of the starting materials in both experiments. More importantly, the increment of the M_s value in the Al_2O_3-5 % komatiite experiment is higher than that in the Al_2O_3-10 % komatiite experiment (Table 2). This trend strongly suggests that the total amount of effective magnetite component in the magnetite–spinel solid solution that was newly generated during serpentinization is greater in the Al_2O_3-5 % komatiite experiment than in the Al_2O_3-10 % komatiite experiment.

Even considering the results of all experiments, the increment of the M_s value decreases with increasing Al_2O_3 content in the starting material, which is likely derived from the decrease in the amount of effective magnetite generated with increasing Al_2O_3 content in the starting material. It is therefore suggested that the increase in Al_2O_3 content in ultramafic rock elevates the amount of smectite and reduces the amount of magnetite in the alteration minerals. The formation of smectite presumably inhibited magnetite formation because the FeO originally contained in the starting material was incorporated directly into smectite.

Effect of Al_2O_3 content in rocks on H_2 concentration in hydrothermal fluid

The three experiments revealed that the final, steady-state H_2 concentrations of fluids were approximately 60 mmol/kg (with olivine), 20 mmol/kg (with Al_2O_3-5 % komatiite), and 0.05 mmol/kg (with Al_2O_3-10 % komatiite) (Figs. 5 and 6; Table 3). The H_2 concentration in the olivine

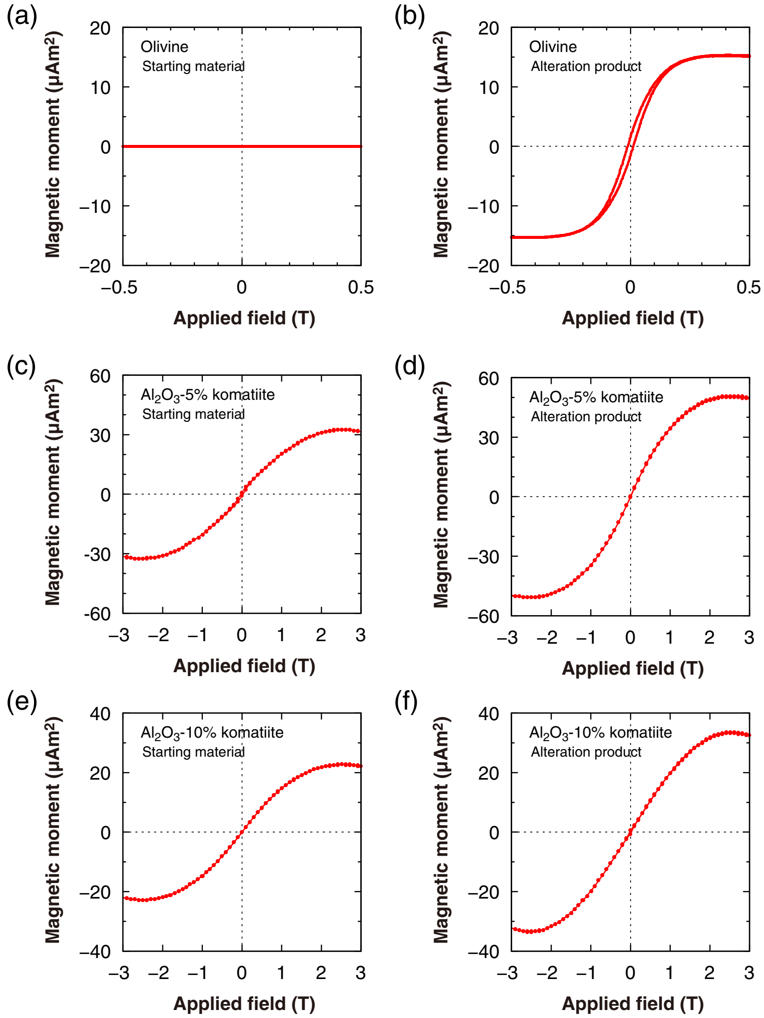

Fig. 3 Magnetic hysteresis loops of (**a**) the starting material and (**b**) the alteration product of the olivine experiment, (**c**) the starting material and (**d**) the alteration product of the Al_2O_3-5 % komatiite experiment, and (**e**) the starting material and (**f**) the alteration product of the Al_2O_3-10 % komatiite experiment. The hysteresis loops were corrected by subtracting diamagnetic/paramagnetic slopes. Note that the loops were measured at 10 K for both komatiite samples and at room temperature for the olivine samples

Table 2 Summary of the magnetic measurements

		Room temperature			10 K			
Experiment	Sample state	*m* (mg)	M_s (µAm²)	M_s (Am²/kg)	*m* (mg)	M_s (µAm²)	M_s (Am²/kg)	T_C (K)
Olivine	Starting material	9.22	0	0	–	–	–	–
	Alteration product	4.14	15.3	3.69	–	–	–	811
Al_2O_3-5 % komatiite	Starting material	11.98	0.62	0.05	33.6	32.1	0.95	~30
	Alteration product	6.58	0.01	0	18.6	50.2	2.70	~30
Al_2O_3-10 % komatiite	Starting material	5.96	0.01	0	41.1	33.0	0.80	~30
	Alteration product	2.70	0.04	0.01	13.1	22.5	1.72	~30

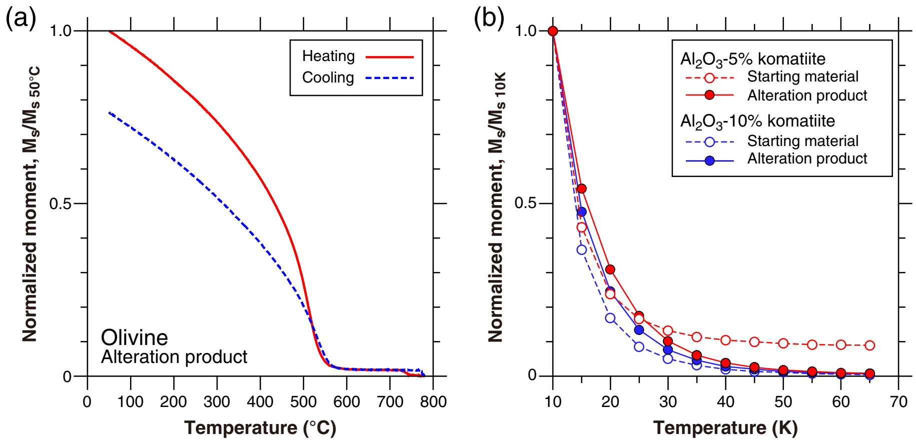

Fig. 4 Results of the Curie temperature measurements. **a** Strong-field thermomagnetic curve for the alteration product of the olivine experiment. **b** Temperature dependency of saturation magnetization of the starting material and alteration product from the Al_2O_3-5 % and Al_2O_3-10 % komatiite experiments, which were calculated from their hysteresis loops measured at various temperatures (e.g., Fig. 3)

experiment is significantly higher than that obtained in a previous experiment with olivine at 400 °C (Allen and Seyfried 2003) and is rather comparable with that generated by an experiment simulating serpentinization of lherzolite at 200 °C (Seyfried et al. 2007). This is consistent with the thermodynamic analysis of serpentinization; olivine becomes stable above approximately 315–390 °C, which limits magnetite formation and H_2 generation in hydrothermal fluid (McCollom and Bach 2009). The steady-state H_2 concentration in the Al_2O_3-5 % komatiite experiment is clearly higher than that obtained from the previous ongoing experiment using Al_2O_3-5 % komatiite and pure water (2.4 mmol/kg) (Yoshizaki et al. 2009). This may be due to the difference of initial solution because NaCl solution is generally much more reactive with rocks than pure water. More importantly, the experiments in this study showed that the steady-state H_2 concentration in fluid increases as the Al_2O_3 content in the starting material is reduced (Fig. 7). This pattern is also consistent with the amount of generated magnetite, which increases with decreasing Al_2O_3 content in the starting material. Therefore, it is suggested that the Al_2O_3 content in the starting material strongly affects the generated H_2 concentration in fluid because the Al_2O_3 level controls the formation of smectite, which potentially inhibits magnetite formation.

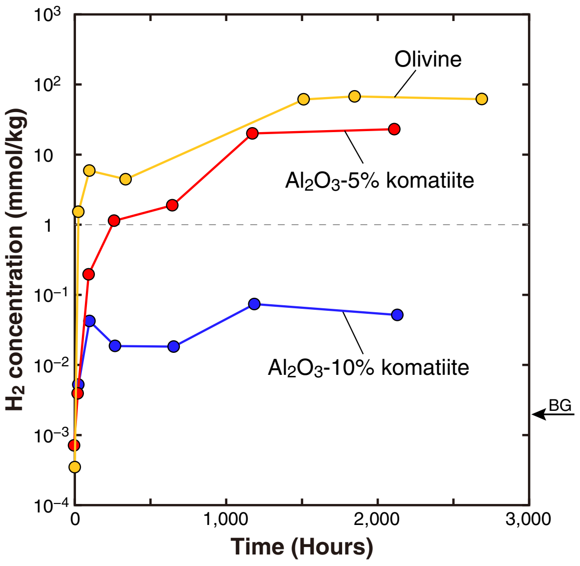

Fig. 5 Changes in H_2 concentration during the experiments with olivine, Al_2O_3-5 % and Al_2O_3-10 % komatiites. The *arrow* indicates the maximum background H_2 concentration after c. 2000 h

Comparison with known H_2 concentrations in modern seafloor hydrothermal vent fluids shows that the concentration in the Al_2O_3-10 % komatiite experiment is comparable to those observed in typical MORB-hosted systems (generally 0.1–1 mmol/kg) (Fig. 6). In contrast, natural peridotite-associated high-temperature hydrothermal fluids have higher H_2 concentrations of up to 16 mmol/kg (Charlou et al. 2002; Gallant and Von Damm 2006; Kumagai et al. 2008), which was successfully reconstructed in experiments using orthopyroxene ± clinopyroxene ± olivine at 400 °C (Allen and Seyfried 2003). Thus, the Al_2O_3-5 % komatiite has the potential to generate an H_2 concentration similar to or higher than those observed in modern peridotite-associated hydrothermal fluids.

Potential role of komatiite serpentinization in the origin of life and early ecosystems in the Hadean ocean

Theoretical predictions for the thermodynamic state of prebiotic chemical evolution have highlighted that the H_2-rich hydrothermal environment is energetically advantageous

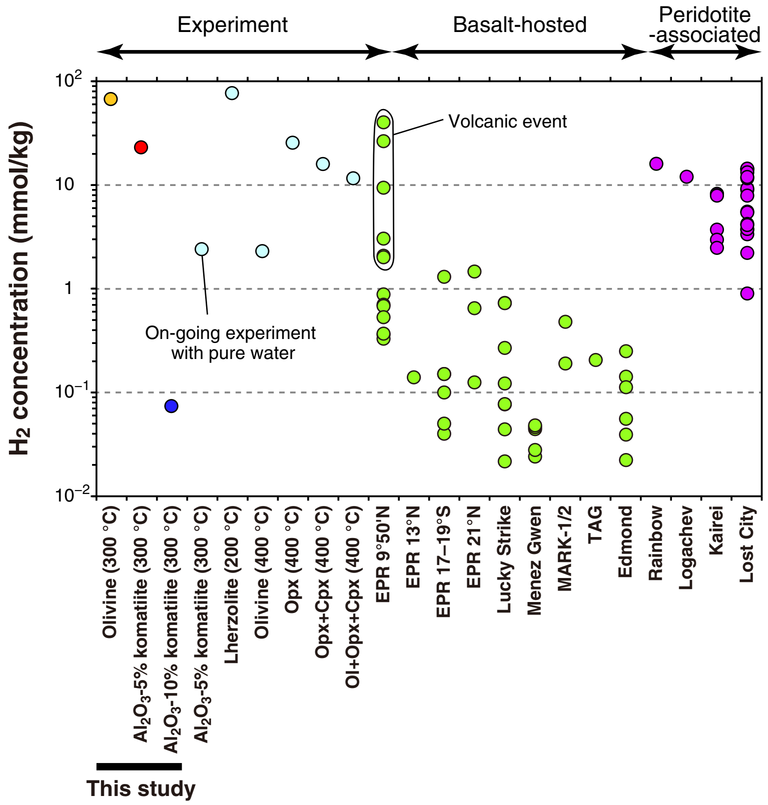

Fig. 6 Comparison of H_2 concentrations in hydrothermal fluid from experiments and modern natural hydrothermal vent systems. Data sources: Al_2O_3-5 % komatiite experiment with pure water at 300 °C and 500 bar (Yoshizaki et al. 2009), lherzolite experiment at 200 °C and 500 bar (Seyfried et al. 2007), four experiments with Ol, Opx, and/or Cpx at 400 °C and 500 bar (Allen and Seyfried 2003), EPR 9°50′N (Lilley et al. 2003; Von Damm and Lilley 2004), EPR 13°N (Von Damm 1995), EPR 17–19°S (Charlou et al. 1996b), EPR 21°S (Lilley et al. 1983), Lucky Strike and Menez Gwen (Charlou et al. 2000), MARK-1/2 (Charlou et al. 2002), TAG (Charlou et al. 1996a), Logatchev and Rainbow (Charlou et al. 2002), Kairei (Gallant and Von Damm 2006; Kumagai et al. 2008), and Lost City (Proskurowski et al. 2006). The H_2 concentrations of seafloor hydrothermal fluids were mainly obtained from the compilation of Nakamura and Takai (2014). Mineral abbreviations: Ol = olivine, Opx = orthopyroxene, Cpx = clinopyroxene

for synthesis and preservation of organic molecules such as amino acids and fatty acids (Amend and McCollom 2009; Amend et al. 2011). Furthermore, it has been hypothesized that the most plausible energy metabolisms to support the emergence and early evolution of life may have been H_2-driven hydrogenotrophic methanogenesis/acetogenesis and/or methanotrophic acetogenesis (Russell et al. 1989; Takai et al. 2006; Martin et al. 2008; Russell et al. 2010, 2014). In this section, we discuss the possible geological settings that may have generated H_2-rich hydrothermal systems in the Hadean ocean.

Considering the relationship between the decreasing mantle temperature during the history of Earth and the

Table 3 Changes in H_2 concentration and pH of fluid samples through time

Olivine			Al_2O_3-5 % komatiite			Al_2O_3-10 % komatiite		
Time (h)	$pH_{25\ °C}$	H_2 (mmol/kg)	Time (h)	$pH_{25\ °C}$	H_2 (mmol/kg)	Time (h)	$pH_{25\ °C}$	H_2 (mmol/kg)
0	6.8	3.5×10^{-4}	0	7.0	7.1×10^{-4}	0	7.0	n.d.
24	10.3	1.5	24	7.5	3.9×10^{-3}	24	7.7	0.005
96	9.6	5.9	96	8.2	0.20	96	7.3	0.042
336	10.9	4.4	264	8.2	1.1	264	7.8	0.019
1512	10.8	61.2	648	7.7	1.9	648	8.5	0.018
1848	10.9	67.4	1176	8.1	20.0	1176	7.5	0.074
2688	10.5	61.8	2112	8.0	23.0	2112	7.7	0.052
						2668	8.0	0.030

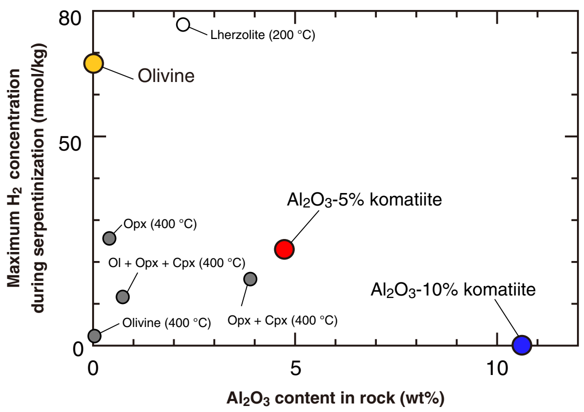

Fig. 7 Relationships between fluid H_2 concentration during serpentinization and Al_2O_3 content in the starting solid material. For comparison, the results of the lherzolite experiment at 200 °C (Seyfried et al. 2007) and the experiments with Ol, Opx, and/or Cpx at 400 °C (Allen and Seyfried 2003) are also shown

chemical composition/production process of komatiites, the different H_2 generation potentials of ADK and AUK imply that komatiite-hosted hydrothermal fluid evolved from H_2-enriched to H_2-depleted through geologic time. Previously, high-pressure experiments on the generation of komatiite melts revealed that ADK melt is generated under high-temperature and high-pressure (>7 GPa) conditions, leaving majoritic garnet as a liquidus phase of mantle, whereas AUK may form owing to high degrees of mantle melting at shallower depths where olivine is a liquidus phase (e.g., Herzberg 1992; Arndt et al. 2008). Therefore, it is believed that the formation of ADK requires a higher mantle plume temperature than for the generation of AUK. This indicates that ADK was produced more abundantly in the oceanic-island/plateau volcanism of the earlier Earth with the hotter mantle than AUK, which is consistent with the geological records of ~3.5 Ga Barberton-type (Al-depleted) and c. 2.7 Ga Munro-type (Al-undepleted) komatiites (Nesbitt et al. 1979; Herzberg 1992). As the Al_2O_3-5 % (Al-depleted) komatiite has a greater potential to enrich H_2 in hydrothermal fluid than Al_2O_3-10 % (Al-undepleted) komatiite (Figs. 6 and 7), the H_2-rich hydrothermal environments hosted by ADK were present abundantly and ubiquitously on the ocean floor prior to the early Archean.

In contrast, the exposure of mantle peridotite at the ocean floor was probably rare in the Archean (Takai et al. 2006). Modern abyssal peridotite is frequently observed near slow-spreading ridges without sufficient magmatic supply because large-scale normal faults (e.g., detachment faults) penetrate deeply, and the mantle peridotite is dragged up to the seafloor (Escartín et al. 2003). However, it has been revealed that the Archean oceanic crust was much thicker than the modern equivalent owing to the higher potential mantle temperature at that time (Moores 2002; Ohta et al. 1996; Komiya 2004; Shibuya et al. 2007, 2012). The thicker ocean crust would have limited the development of deep normal faults reaching to the mantle and exposure of mantle peridotite, which has led to the hypothesis that the early Archean H_2-rich hydrothermal environment was mainly driven by komatiite volcanism instead of much less abundant fault-related peridotite (Takai et al. 2006). This hypothesis is further substantiated by the results obtained in this study and can be applied to the Hadean. The serpentinization of ADK may have generated abundant H_2-rich (ca. 20 mmol/kg) hydrothermal fluid and proximal H_2-rich hydrothermal fluid–seawater mixing zones in the Hadean ocean, which could potentially have served as nurseries for prebiotic chemical evolution and the subsequent emergence and early evolution of life on Earth. Furthermore, considering that the oceanic crust was probably sufficiently thick throughout the Hadean and Archean to limit the exposure of peridotite on the seafloor and that ADK disappeared after the early Archean, the Hadean era was more favorable for the emergence of life than the Archean era in terms of H_2-rich hydrothermal environments.

Conclusions

The H_2 generation potential of ADK and AUK during serpentinization was estimated by the experimental hydrothermal reactions of komatiites at 300 °C and 500 bar. The experiments revealed that the H_2 concentration (ca. 20 mmol/kg) in hydrothermal fluid generated from the serpentinization of ADK is comparable to that of the most H_2-rich hydrothermal systems in modern oceans. Furthermore, considering the limited exposure of mantle peridotite owing to the thick lid of oceanic crusts in the Hadean ocean floor, ADK was likely the most ubiquitous seafloor ultramafic rock that could host H_2-rich hydrothermal system. Such H_2-rich hydrothermal systems would have provided a favorable environment (redox, electrochemical, and thermal gradients in the seawater/hydrothermal fluid mixing zone) for the acquisition of bioavailable free energy and for prebiotic chemical evolution in the Hadean. Further experiments and thermodynamic calculations to simulate the mixing between Hadean seawater and H_2-rich hydrothermal fluid should be carried out to test this hypothesis.

Competing interests

The authors declare that they have no competing interests.

Authors' contributions

TS, KN, KT, and SM proposed and designed the study. TS and MY carried out the experiments. TS, MY, and KS prepared the starting materials. TS, MY, MS, and HT analyzed the fluid samples and solid materials. TS, MY, MS, KN, SO, KS, and KT interpreted the data. All authors read and approved the final manuscript.

Acknowledgements
We thank the three anonymous reviewers for their helpful comments and H Kawahata for careful editorial handling. This study was partially supported by the Trans-crustal Advection and In-situ biogeochemical processes of Global sub-seafloor Aquifer (TAIGA) project and the Grants-in-Aid for Scientific Research (No. 22740333) from the Japanese Ministry of Education, Culture, Sports, Science and Technology. This work was also performed under the cooperative research program of Center for Advanced Marine Core Research (CMCR), Kochi University (Accept No. 14A007 and 14B005).

Author details
[1]Laboratory of Ocean-Earth Life Evolution Research (OELE), Japan Agency for Marine-Earth Science and Technology (JAMSTEC), 2-15 Natsushima-cho, Yokosuka 237-0061, Japan. [2]Research and Development (R&D) Center for Submarine Resources, Japan Agency for Marine-Earth Science and Technology (JAMSTEC), 2-15 Natsushima-cho, Yokosuka 237-0061, Japan. [3]Project Team for Development of New-generation Research Protocol for Submarine Resources, Japan Agency for Marine-Earth Science and Technology (JAMSTEC), 2-15 Natsushima-cho, Yokosuka 237-0061, Japan. [4]Department of Earth and Planetary Sciences, Tokyo Institute of Technology, 2-12-1 Ookayama, Meguro-ku, Tokyo 152-8551, Japan. [5]Geological Survey of Japan, National Institute of Advanced Industrial Science and Technology, 1-1-1 Higashi, Tsukuba 305-8567, Japan. [6]Kochi Institute for Core Sample Research, Japan Agency for Marine-Earth Science and Technology (JAMSTEC), 200 Monobe, Nankoku, Kochi 783-8502, Japan. [7]Department of Systems Innovation, The University of Tokyo, 7-3-1 Hongo, Bunkyo-ku, Tokyo 113-8656, Japan. [8]The Open University of Japan, 2-11 Wakaba, Mihama-ku, Chiba 261-8586, Japan. [9]Department of Subsurface Geobiological Analysis and Research (SUGAR), Japan Agency for Marine-Earth Science and Technology (JAMSTEC), 2-15 Natsushima-cho, Yokosuka 237-0061, Japan. [10]Earth-Life Science Institute, Tokyo Institute of Technology, 2-12-1 Ookayama, Meguro-ku, Tokyo 152-8551, Japan.

Received: 10 July 2015 Accepted: 8 December 2015

References

Allen DE, Seyfried Jr WE. Compositional controls on vent fluids from ultramafic-hosted hydrothermal systems at midocean ridges: an experimental study at 400 °C, 500 bars. Geochim Cosmochim Acta. 2003;67:1531–42.

Amend JP, McCollom TM. Energetics of biomolecule synthesis on early Earth. In: Zaikowski L, Friedrich JM, Seidel SR, editors. Chemical evolution II: from the origins of life to modern society. Washington, D.C.: American Chemical Society; 2009. p. 63–94.

Amend JP, McCollom TM, Hentscher M, Bach W. Catabolic and anabolic energy for chemolithoautotrophs in deep-sea hydrothermal systems hosted in different rock types. Geochim Cosmochim Acta. 2011;75:5736–48.

Arndt N, Ginibre C, Chauvel C, Albarède F, Cheadle M, Herzberg C, et al. Were komatiites wet? Geology. 1998;26:739–42.

Arndt N, Lesher CM, Barnes SJ. Komatiite. Cambridge: Cambridge University Press; 2008.

Arth JG, Arndt NT, Naldrett AJ. Genesis of Archean komatiites from Munro Township, Ontario: trace-element evidence. Geology. 1977;5:590–4.

Berry AJ, Danyushevsky LV, O'Neill HSC, Newville M, Sutton SR. Oxidation state of iron in komatiitic melt inclusions indicates hot Archaean mantle. Nature. 2008;455:960–3.

Campbell IH, Griffiths RW, Hill RI. Melting in an Archean mantle plume—heads its basalts, tails its komatiites. Nature. 1989;339:697–9.

Canil D. Vanadium partitioning and the oxidation state of Archaean komatiite magma. Nature. 1997;389:842–5.

Canil D. Vanadium partitioning between orthopyroxene, spinel and silicate melt and the redox states of mantle source regions for primary magmas. Geochim Cosmochim Acta. 1999;63:557–72.

Charlou JL, Donval JP, Jean-Baptiste P, Dapoigny A, Rona PA. Gases and helium isotopes in high temperature solutions sampled before and after ODP Leg 158 drilling at TAG hydrothermal field (26°N, MAR). Geophys Res Lett. 1996a;23:3491–4.

Charlou JL, Fouquet Y, Donval JP, Auzende JM, Jean-Baptiste P, Stievenard M, et al. Mineral and gas chemistry of hydrothermal fluids on an ultrafast spreading ridge: East Pacific Rise, 17° to 19°S (Naudur cruise, 1993) phase separation processes controlled by volcanic and tectonic activity. J Geophys Res. 1996b; 101:15899–919.

Charlou JL, J. P. Donval a ED, Jean-Baptiste P, Radford-Knoery J, Fouquet Y, Dapoigny A, et al. Compared geochemical signatures and the evolution of Menez Gwen (37°50′N) and Lucky Strike (37°17′N) hydrothermal fluids, south of the Azores Triple Junction on the Mid-Atlantic Ridge. Chem Geol. 2000;171:49–75.

Charlou JL, Donval JP, Fouquet Y, Jean-Baptiste P, Holm N. Geochemistry of high H_2 and CH_4 vent fluids issuing from ultramafic rocks at the Rainbow hydrothermal field (36°14′N, MAR). Chem Geol. 2002;191:345–59.

Escartín J, Mével C, MacLeod CJ, McCaig AM. Constraints on deformation conditions and the origin of oceanic detachments: the Mid-Atlantic Ridge core complex at 15°45′N. Geochem Geophy Geosy. 2003;4:1067. doi:10.1029/2002GC000472.

Gallant RM, Von Damm KL. Geochemical controls on hydrothermal fluids from the Kairei and Edmond Vent Fields, 23°–25°S, Central Indian Ridge. Geochem Geophy Geosy. 2006;7:Q06018. doi:10.01029/02005GC001067.

Grove TL, Parman SW. Thermal evolution of the Earth as recorded by komatiites. Earth Planet Sci Lett. 2004;219:173–87.

Harrison RJ, Putnis A. Magnetic properties of the magnetite-spinel solid solution: curie temperature, magnetic susceptibilities, and cation ordering. Am Mineral. 1996;81:375–84.

Herzberg C. Depth and degree of melting of komatiites. J Geophys Res. 1992;97:4521–40.

Herzberg C, Condie K, Korenaga J. Thermal history of the Earth and its petrological expression. Earth Planet Sci Lett. 2010;292:79–88.

Hsu H-W, Postberg F, Sekine Y, Shibuya T, Kempf S, Horányi M, et al. Ongoing hydrothermal activities within Enceladus. Nature. 2015;519:207–10.

Hunt CP, Moskowitz BM, Banerjee SK. Magnetic properties of rocks and minerals. In: Ahrens TJ, editor. Rock physics & phase relations: a handbook of physical constants. Washington, D. C.: American Geophysical Union; 1995. p. 189–204.

Inoue T, Sawamoto H. High pressure melting of pyrolite under hydrous condition and its geophysical implication. In: Syono Y, Manghnani MH, editors. High-pressure research: application to earth and planetary sciences. Washington D. C.: Terra, Tokyo and AGU; 1992. p. 323–31.

Inoue T, Rapp RP, Zhang J, Gasparik T, Weidner DJ, Irifune T. Garnet fractionation in a hydrous magma ocean and the origin of Al-depleted komatiites: melting experiments of hydrous pyrolite with REEs at high pressure. Earth Planet Sci Lett. 2000;177:81–7.

Janecky DR, Seyfried Jr WE. Hydrothermal serpentinization of peridotite within the oceanic crust: experimental investigations of mineralogy and major element chemistry. Geochim Cosmochim Acta. 1986;50:1357–78.

Kato S, Shibuya T, Nakamura K, Suzuki K, Rejishkumar VJ, Yamagishi A. Elemental dissolution of basalts with ultra-pure water at 340 °C and 40 MPa in a newly developed flow-type hydrothermal apparatus. Geochem J. 2013;47:89–92.

Kelley DS, Karson JA, Blackman DK, Früh-Green GL, Butterfield DA, Lilley MD, et al. An off-axis hydrothermal vent field near the Mid-Atlantic Ridge at 30°N. Nature. 2001;412:145–9.

Kelley DS, Karson JA, Früh-Green GL, Yoerger DR, Shank TM, Butterfield DA, et al. A serpentinite-hosted ecosystem: the Lost City hydrothermal field. Science. 2005;307:1428–34.

Knauth LP. Temperature and salinity history of the Precambrian ocean: implications for the course of microbial evolution. Palaeogeogr Palaeoclimateol Palaeoecol. 2005;219:53–69.

Komiya T. Material circulation model including chemical differentiation within the mantle and secular variation of temperature and composition of the mantle. Phys Earth Planet Inter. 2004;146:333–67.

Kumagai H, Nakamura K, Toki T, Morishita T, Okino K, Ishibashi J-i, et al. Geological background of the Kairei and Edmond hydrothermal fields along the Central Indian Ridge: implications of their vent fluids' distinct chemistry. Geofluids. 2008;8:239–51.

Lang SQ, Butterfield DA, Schulte M, Kelley DS, Lilley MD. Elevated concentrations of formate, acetate and dissolved organic carbon found at the Lost City hydrothermal field. Geochim Cosmochim Acta. 2010;74:941–52.

Lazar C, McCollom TM, Manning CE. Abiogenic methanogenesis during experimental komatiite serpentinization: implications for the evolution of the early Precambrian atmosphere. Chem Geol. 2012;326–327:102–12.

Lilley MD, Baross JA, I GL. Reduced gases and bacteria in hydrothermal fluids: the Galapagos spreading center and 21°N East Pacific Rise. In: Rona PA, Bostrom K, Laubier L, Smith Jr KL, editors. Hydrothermal processes at seafloor spreading centers. Marine Sciences: NATO Conference Series IV; 1983. p. 411–49.

Lilley MD, Butterfield DA, Lupton JE, Olson EJ. Magmatic events can produce rapid changes in hydrothermal vent chemistry. Nature. 2003;422:878–81.

Martin W, Baross J, Kelley D, Russell MJ. Hydrothermal vents and the origin of life. Nat Rev Microbiol. 2008;6:805–14.

McCollom TM, Bach W. Thermodynamic constraints on hydrogen generation during serpentinization of ultramafic rocks. Geochim Cosmochim Acta. 2009;73:856–75.

McCollom TM, Sherwood Lollar B, Lacrampe-Couloume G, Seewald JS. The influence of carbon source on abiotic organic synthesis and carbon isotope fractionation under hydrothermal conditions. Geochim Cosmochim Acta. 2010;74:2717–40.

Moores EM. Pre-1 Ga (pre-Rodinian) ophiolites: their tectonic and environmental implications. Geol Soc Am Bull. 2002;114:80–95.

Morishita T, Nakamura K, Shibuya T, Kumagai H, Sato T, Okino K, et al. Petrology of peridotites and related gabbroic rocks around the Kairei hydrothermal field in the Central Indian Ridge. In: Ishibashi J, Okino K, Sunamura M, editors. Subseafloor biosphere linked to hydrothermal systems. Tokyo: Springer Japan; 2015. p. 177–93.

Nakamura K, Morishita T, Bach W, Klein F, Hara K, Okino K, et al. Serpentinized troctolites exposed near the Kairei Hydrothermal Field, Central Indian Ridge: insights into the origin of the Kairei hydrothermal fluid supporting a unique microbial ecosystem. Earth Planet Sci Lett. 2009;280:128–36.

Nakamura K, Takai K. Theoretical constraints of physical and chemical properties of hydrothermal fluids on variations in chemolithotrophic microbial communities in seafloor hydrothermal systems. Prog Earth Planet Sci. 2014;1:5. doi:10.1186/2197-4284-1-5.

Nesbitt RW, Sun SS, Purvis AC. Komatiites: geochemistry and genesis. Can Mineral. 1979;17:165–86.

Ohta H, Maruyama S, Takahashi E, Watanabe Y, Kato Y. Field occurrence, geochemistry and petrogenesis of the Archean mid-oceanic ridge basalts (AMORBs) of the Cleaverville area, Pilbara Craton, Western Australia. Lithos. 1996;37:199–221.

Proskurowski G, Lilley MD, Kelley DS, Olson EJ. Low temperature volatile production at the Lost City hydrothermal field, evidence from a hydrogen stable isotope geothermometer. Chem Geol. 2006;229:331–43.

Puchtel IS, Blichert-Toft J, Touboul M, Walker RJ, Byerly GR, Nisbet EG, et al. Insights into early Earth from Barberton komatiites: evidence from lithophile isotope and trace element systematics. Geochim Cosmochim Acta. 2013;108:63–90.

Russell MJ, Hall AJ, Turner D. In vitro growth of iron sulphide chimneys: possible culture chambers for origin-of-life experiments. Terra Nova. 1989;1:238–41.

Russell MJ, Hall AJ, Martin W. Serpentinization as a source of energy at the origin of life. Geobiology. 2010;8:355–71. doi:10.1111/j.1472-4669.2010.00249.x.

Russell MJ, Barge L, Bhartia R, Bocanegra D, Bracher P, Branscomb E, et al. The drive to life on wet and icy worlds. Astrobiology. 2014;14:308–43.

Sekine Y, Shibuya T, Postberg F, Hsu H-W, Suzuki K, Masaki Y, et al. High-temperature water–rock interactions and hydrothermal environments in the chondrite-like core of Enceladus. Nat Commun. 2015;6:8604. doi:10.1038/ncomms9604.

Seyfried Jr WE, Gordon PC, Dickson FW. A new reaction cell for hydrothermal solution equipment. Am Mineral. 1979;64:646–9.

Seyfried Jr WE. Experimental and theoretical constraints on hydrothermal alteration processes at mid-ocean ridges. Annu Rev Earth Planet Sci. 1987;15:317–35.

Seyfried Jr WE, Foustoukos DI, Fu Q. Redox evolution and mass transfer during serpentinization: an experimental and theoretical study at 200 °C, 500 bar with implications for ultramafic-hosted hydrothermal systems at mid-ocean ridges. Geochim Cosmochim Acta. 2007;71:3872–86.

Shibuya T, Kitajima K, Komiya T, Terabayashi M, Maruyama S. Middle Archean ocean ridge hydrothermal metamorphism and alteration recorded in the Cleaverville area, Pilbara Craton, Western Australia. J Metamorph Geol. 2007;25:751–67.

Shibuya T, Komiya T, Nakamura K, Takai K, Maruyama S. Highly alkaline, high-temperature hydrothermal fluids in the early Archean ocean. Precambrian Res. 2010;182:230–8.

Shibuya T, Tahata M, Kitajima K, Ueno Y, Komiya T, Yamamoto S, et al. Depth variation of carbon and oxygen isotopes of calcites in Archean altered upper oceanic crust: implications for the CO_2 flux from ocean to oceanic crust in the Archean. Earth Planet Sci Lett. 2012;321–322:64–73.

Shibuya T, Yoshizaki M, Masaki Y, Suzuki K, Takai K. Reactions between basalt and CO_2-rich seawater at 250 and 350 °C, 500 bars: implications for the CO_2 sequestration into the modern oceanic crust and the composition of hydrothermal vent fluid in the CO_2-rich early ocean. Chem Geol. 2013;359:1–9.

Shimizu K, Komiya T, Hirose K, Shimizu N, Maruyama S. Cr-spinel, an excellent micro-container for retaining primitive melts – implications for a hydrous plume origin for komatiites. Earth Planet Sci Lett. 2001;189:177–88.

Sleep NH, Bird DK, Pope EC. Serpentinite and the dawn of life. Philos Trans R Soc Lond B Biol Sci. 2011;366:2857–69.

Suzuki K, Kato S, Shibuya T, Hirose T, Fuchida S, Kumar YR, et al. Development of hydrothermal and frictional experimental systems to simulate sub-seafloor water–rock–microbe interactions. In: Ishibashi J, Okino K, Sunamura M, editors. Subseafloor biosphere linked to hydrothermal systems. Tokyo: Springer Japan; 2015a. p. 71–85.

Suzuki K, Shibuya T, Yoshizaki M, Hirose T. Experimental hydrogen production in hydrothermal and fault systems: significance for habitability of subseafloor H_2 chemoautotroph microbial ecosystems. In: Ishibashi J, Okino K, Sunamura M, editors. Subseafloor Biosphere Linked to Hydrothermal Systems. Tokyo: Springer Japan; 2015b. p. 87–94.

Takahashi E, Scarfe CM. Melting of peridotite to 14 GPa and the genesis of komatiites. Nature. 1985;315:566–8.

Takai K, Nakamura K, Suzuki K, Inagaki F, Nealson KH, Kumagai H. Ultramafics-Hydrothermalism-Hydrogenesis-HyperSLiME (UltraH3) linkage: a key insight into early microbial ecosystem in the Archean deep-sea hydrothermal systems. Paleontol Res. 2006;10:269–82.

Viljoen MJ, Viljoen RP. Evidence for the existence of a mobile extrusive peridotitic magma from the Komati Formation of the Onverwacht Group. Geol Soc S Afr Spec Publ. 1969;2:87–113.

Von Damm KL. Controls on the chemistry and temporal variability of seafloor hydrothermal fluids. In: Humphris SE, Zierenberg RA, Mullineaux LS, Thomson RE, editors. Seafloor hydrothermal systems: physical, chemical, biological, and geological interactions. Washington DC: Geophysical Monograph. American Geophysical Union; 1995. p. 222–47.

Von Damm KL, Lilley MD. Diffuse flow hydrothermal fluids from 9°50′N East Pacific Rise: origin, evolution and biogeochemical controls. In: Wilcock WSD, DeLong EF, Kelley DS, Baross JA, Cary SC, editors. The subseafloor biosphere at mid-ocean ridges, Geophysical Monograph, vol. 144. Washington DC: American Geophysical Union; 2004. p. 245–68.

Wei K, Tronnes RG, Scarfe CM. Phase relations of aluminum-undepleted and aluminum-depleted komatiites at pressures of 4–12 GPa. J Geophys Res. 1990;95:15817–27.

Wetzel LR, Shock EL. Distinguishing ultramafic- from basalt-hosted submarine hydrothermal systems by comparing calculated vent fluid compositions. J Geophys Res. 2000;105:8319–40.

Yoshizaki M, Shibuya T, Suzuki K, Shimizu K, Nakamura K, Takai K, et al. H_2 generation by experimental hydrothermal alteration of komatiitic glass at 300 °C and 500 bars: a preliminary result from on-going experiment. Geochem J. 2009;43:e17–22.